IEEE Access
Multidisciplinary | Rapid Review | Open Access Journal

Received July 21, 2019, accepted August 3, 2019, date of publication August 7, 2019, date of current version September 10, 2019.

Digital Object Identifier 10.1109/ACCESS.2019.2933740

The Dependence of Microstructural Evolution and Corrosion Resistance of a Sandwich Multi-Layers Brazing Sheets on the Homogenization Annealing

ZHIPENG YUAN[1,2], FANGYUN TAO[3], JIE WEN[1,2], AND YIYOU TU[1,2]

[1]School of Materials Science and Engineering, Southeast University, Nanjing 211189, China
[2]Jiangsu Key Laboratory of Advanced Metallic Materials, Southeast University, Nanjing 211189, China
[3]Department of Applied Mathematics, College of Science, Nanjing Forestry University, Nanjing 210037, China

Corresponding author: Yiyou Tu (tuyiyou@seu.edu.cn)

This work was supported by the Jiangsu Science and Technology Department under Grant 7712000055.

ABSTRACT The influence of the microstructure on the corrosion susceptibility and mechanism of aluminum sheet was studied. The homogenization annealing treatment results in the segregation of copper on the surface of the re-solidified clad material and the increase of the diffusion depth of Si during brazing. The band of dense precipitates has a higher corrosion potential than clad and core material, and the high density particles in the diffusion zone (40 um<depth<70 um) are identified as α-Al(Fe-Mn)Si particles. Thus, the band of dense precipitates are catalytic sites for cathodic reduction reactions. Moreover, the effect of homogenization annealing treatment on the local electrochemical activity and corrosion properties are studied. The results indicate that the band of dense precipitates formed in the diffusion zone in the sample without homogenization annealing during brazing process, which improves the corrosion resistance of the material. Compared with sample with homogenization annealing at the same thickness, the time for the perforation during seawater acetic acid test of the sample without homogenization is longer than that of the homogenization annealed sample.

INDEX TERMS Aluminum brazing sheet, microstructural characterization, Si diffusion, electrochemical characterization, corrosion behavior.

I. INTRODUCTION

Aluminum alloys are commonly used in automotive applications due to their light weight and excellent physical properties [1]–[4]. During the complex manufacturing of heat exchanger tubes, the interdependence between the evolution of the microstructure and the processes at each stage become increasingly important. To improve the mechanical properties and corrosion resistance of brazing sheets, it is a good way to optimize components by thermo-mechanical processing [5]–[8]. Microstructural evolution depends not only on the alloy composition, but also on the process conditions to a large extent. Thus, homogenization annealing conditions, one of the important parts of brazing sheets manufacture process, should be carefully considered.

Homogenizing heat treatment of the material reduces the concentration of Mn in solid solution and is used to change the size and the distribution of the particles [9]. During homogenization, the composition and morphology of the primary phase change, and the secondary particles initially precipitate and subsequently dissolve. The homogenized microstructure may greatly affect the recrystallization behavior, grain size, mechanical properties and corrosion resistance of the final product [9].

D Different sizes of precipitated particles form during the homogenization annealing process, and they may influence the evolution of microstructure and texture [10]. Large particles (>1 or 2μm) promote recrystallization, and finely dispersed particles (<1μm) inhibit recrystallization [11]. It has been reported that the precipitation that occurs before recrystallization during annealing can greatly retard the onset of recrystallization and affect recrystallized grain structure [12], [13]. Humphreys and Hatherly pointed out the effect of strong solute on the recovery process and its influence the recrystallization driving pressure [14].

The corrosion resistance of heat exchanger materials is commonly measured through seawater acetic acid test (SWAAT). Several studies have focused on the corrosion

The associate editor coordinating the review of this manuscript and approving it for publication was Ildiko Peter.

behavior of Al brazing sheet material. Afshar *et al.* found that α-Al(Fe,Mn)Si particles on the surface will increase the cathode current density of the re-solidified clad [15], [16]. Copper was added to the core of brazing sheets, which greatly improves the corrosion life of the material [17].

The research is dedicated to improving the corrosion resistance of aluminum brazing sheet. The microstructure and element distribution of the materials before and after brazing were studied by optical microscopy (OM), scanning electron microscope (SEM) and electron probe X-ray micro analysis (EPMA). The open circuit potential of aluminum brazing sheet as a function of depth after brazing is measured. The present work aims to investigate the effect of homogenization heat treatment on the corrosion performance of AA4343/3z23a/AA4343 layered aluminum brazing sheets and provide enhanced corrosion protection by microstructural control of the aluminum brazing sheet.

II. EXPERIMENTAL

A. MATERIALS

The experimental material was a sandwich multi-layers AA4343/3z23a/AA4343 brazing aluminum sheet with a thickness of 0.27 mm. Its chemical composition is presented in Table 1.

TABLE 1. Chemical composition (wt. %) of 3z23a (core) and AA4343 (clad) materials.

	Si	Fe	Cu	Mn	Zn	Ti	Al
Clad 4343	8.0	0.25	0.05	0.06	0.03	0.1	Bal.
Core 3z23a	0.046	0.245	0.337	1.45	0.002	0.143	Bal.

As are listed in Table 2, the layered aluminum sheets were divided into two parts and denoted as A and B.

TABLE 2. Different homogenization annealing treatments of layered aluminum sheets.

Material	Processing	Homogenization annealing treatment
AA4343/3z23a/AA4343 layered aluminum sheets	A	No homogenization annealing
	B	Homogenization annealing at 590°C within 15 h, held at this temperature for 17 h and air-cooled to room temperature.

B. BRAZING PRODUCEDURE

The sheets were properly placed in a controlled atmosphere brazing furnace and were heated to 600°C within 15 minutes, held at this temperature for 5 min and cooled to room temperature at a specified ramp (100°C/min).

C. FLUIDITY TEST OF THE CLAD MATERIAL

At present, no test method for evaluating the fluidity of the clad material is available. In this paper, a method for testing the fluidity of the clad material by jiangsu Alcha Aluminum Company Ltd. was adopted. Testing process for clad fluidity is shown in Table 3. The K value was used to characterize the fluidity of the brazing layer, mainly depending on W_b, W_o and Cl_r. The K value can be calculated as follows:

$$K = \frac{W_b - 0.25 \times W_0}{0.75 \times W_0 \times Cl_r} \quad (1)$$

where W_o is the total weight of the sample after brazing, W_b is the weight of the bottom quarter of the sample after brazing, and Cl_r is the total cladding rate. When $K \geq 0.2$, the fluidity of the brazing layer meets the requirements.

TABLE 3. Process for the fluidity test.

	Step 1	Step 2	Step 3	Step 4
Temperature	20-600°C	600°C	600-570°C	570-20°C
Time	17 min	10 min	Furnace cooling	Air cooling

D. MICROSTRUCTURAL ANALYSIS

The microstructures of the sheets were examined before and after brazing by OM, SEM and EPMA. EPMA provided quantitative line scans of Si and Cu before and after brazing.

E. ELECTROCHEMICAL ANALYSIS

The electrochemical properties of the sheets with and without homogenization were investigated by corrosion potential measurements and the cathodic and the anode polarization measurements. The electrolyte was a 3.5 wt.% NaCl solution acidified to pH 2.8 by adding acetic acid.

The specimens were cut into pieces approximately 15 mm×100 mm in size and degreased with acetone. The sample was covered with 704 silicone rubber with a window size of 10 mm×10 mm on the clad side. Electrochemical tests were performed in an environment with no stirring. The corrosion potential under open circuit condition for samples was recorded for 1 h.

F. CORROSION ATTACK MECHANISM

SWAAT samples of 60 mm×60 mm were used. The back side and edges were covered with 3M Scotch brand tape M470 [18] During the experiment, the conditions inside the cabinet were kept constant. The spray was 3.5 wt. % of sodium chloride acidified with glacial acetic acid. The pH was then adjusted to 2.8 by using 10 wt. % NaOH.

III. RESULTS

A. MICROSTRUCTURAL EVOLUTION

1) OPTICAL MICROSCOPY

The optical microstructures of the cross-sections of the material with and without homogenization annealing before and after brazing are shown in Fig. 2. Before brazing, the clad

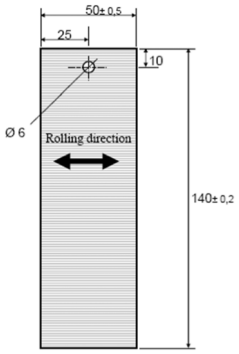

FIGURE 1. Schematic of the sheet. All dimensions in mm.

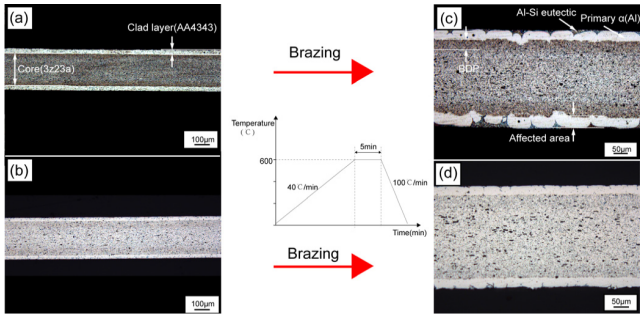

FIGURE 2. Optical images of the brazing sheets with a thickness 0.27 mm with and without homogenization annealing: (a and c): processing A; (b and d): processing B.

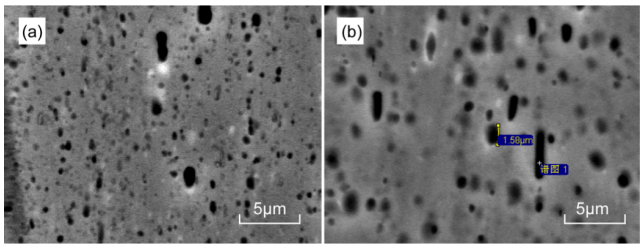

FIGURE 3. SEM images of the sheets with a thickness 0.27 mm before the final annealing. (a) Processing A, (b) Processing B.

material consisted of α-Al matrix and Si particles. The Fe/Mn-containing particles are dispersed in the core material. After brazing, the Al–Si eutectic phase accumulated on the surface and grain boundaries of the re-solidified clad. As shown in Fig. 2(c), for the brazing sheets without homogenization annealing, a 50–60 μm wide Band of Dense Precipitates (BDP) was formed between the liquid clad and solid core.

From Fig. 3(a), without homogenization annealing sample contains more particles, and most of them are smaller than 1 μm. From Fig. 3(b), the sample with homogenization annealing at 590°C contains large-sized particles. During the subsequent annealing, the particles grow and form a large number of particles which are larger than 1 μm.

From Fig. 4, without homogenization annealing sample contains pancake-like recrystallization grains after brazing,

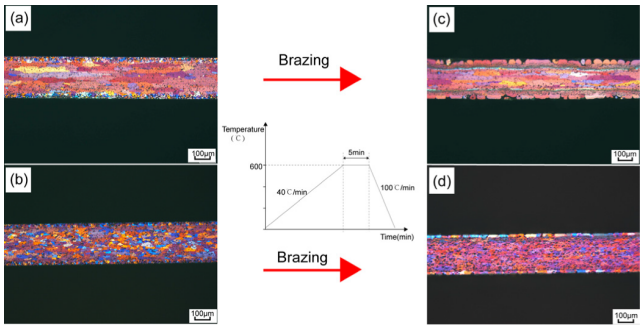

FIGURE 4. Polarized optical images of the brazing sheets with a thickness 0.27 mm with and without homogenization annealing. (a and c) Processing A, (b and d) Processing B.

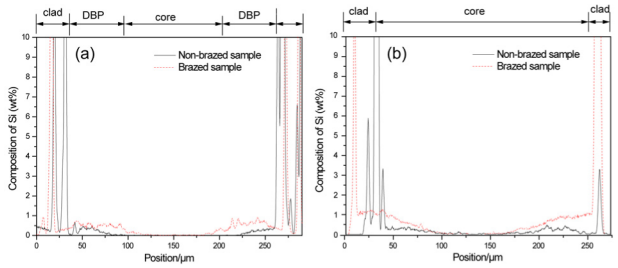

FIGURE 5. EPMA line scan analysis of Si element. (a) Processing A, (b) Processing B.

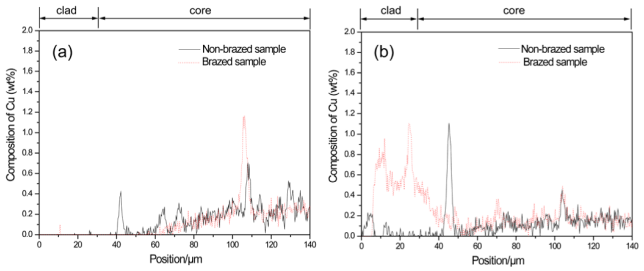

FIGURE 6. EPMA line scans analysis of Cu element. (a) Processing A, (b) Processing B.

and the sample with homogenization annealing contains equiaxed recrystallization grains.

2) EPMA

The EPMA line scans for Si throughout the cross section of the non-brazed and brazed materials are shown in Fig. 5.

From Fig. 5, the concentration of Si in the diffusion zone after brazing shows a significant increase. The quantitative compositional analysis of the elemental distribution in the brazing sheet structure shows that the Si content in the diffusion zone increased by 0.2 wt. % in Processing A (Fig. 5(a)) and 0.6 wt.% in Processing B (Fig. 5(b)). There is a sharp transition from the Si composition in the clad layer to that of the core layer before brazing. From Fig. 5, the diffusion depth of Si in sample B is significantly deeper than that in sample A after brazing.

For non-homogenization annealed samples in Fig. 6(a), Cu in core layer hardly transfers into the clad material before and after brazing. For with homogenization annealing

TABLE 4. The fluidity of the clad material.

Alloy sheet	Cl_r	*Wb*/mg	*Wo*/mg	*K*
Processing A	0.2	5.07	1.30	0.05
Processing B	0.2	5.12	1.49	0.27

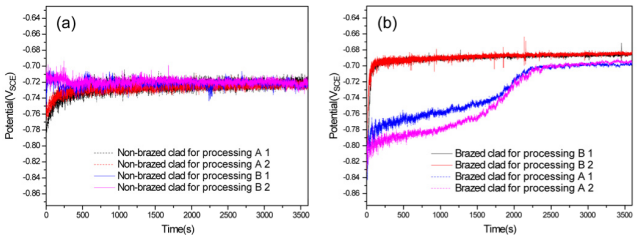

FIGURE 7. Average open-circuit corrosion potentials of non-brazed and brazed clad materials for processing A and B subjected to 1 h of immersion into 3.5 wt.% NaCl solution at pH 2.8 before anodic and cathodic polarization(scan rate 5 mV/s).

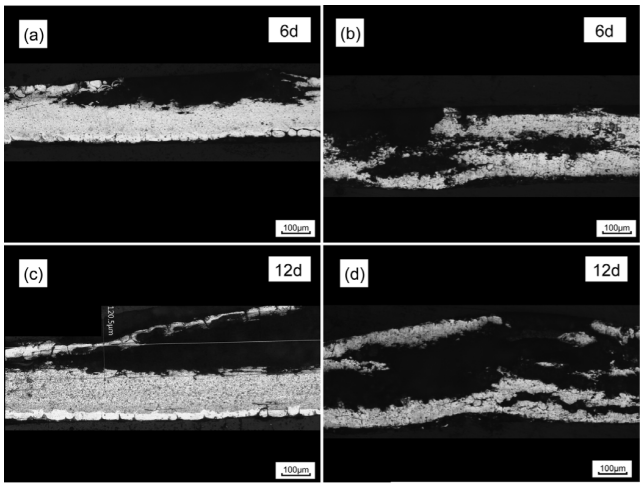

FIGURE 8. The corrosion morphology of brazed material after in SWAAT solution. (a and c) Processing A, (b and d) Processing B.

samples in Fig. 6(b), Cu diffuses into the clad material before brazing. After brazing, the Cu content in the diffusion zone significantly increased. The quantitative analysis reveals an increase of 0.7 wt. % Cu in the diffusion zone.

B. FLUIDITY TEST OF THE CLAD MATERIAL

The calculated K values are presented in Table 4. The calculated K values of the sheets with and without homogenization are 0.05 and 0.27 respectively. Thus, the fluidity of the brazing layer without homogenization is significantly better than that with homogenization.

C. ELECTROCHEMICAL CHARACTERIZATION

The corrosion potentials of the samples with and without homogenization were compared and correlated to the microstructural changes due to homogenization. From Figure 7(a), almost no difference in the open circuit potential (OCP) of clad material was observed with and without homogenization for the non-brazed material. For the clad material with homogenization, 10-mV increase of the open-circuit corrosion potential are observed after brazing.

D. CORROSION MORPHOLOGY

Fig. 8 shows the corrosion morphology of the brazed material after 6 and 12 days in SWAAT solution. From Fig. 8(b), sample B has been almost penetrated after 6 days SWAAT, while only partial exfoliation was observed in sample A (Fig.8(a)). As shown in Fig. 8(c), the residual clad of sample A is partly exfoliated because of the corrosion of the diffusion region. When the corrosion spread to the BDP, the corrosion form is replaced by exfoliation corrosion due to the lower corrosion potential of the dense precipitates (Al(Fe,Mn)Si phase).

IV. DISCUSSION

A. MICROSTRUCTURAL ANALYSIS

The second phase particles strongly influence the recrystallization kinetics and final grain size. Based on SEM images in Fig. 3(a), small dispersed second phase particles in non-homogeneous annealing sample strongly affect the simultaneous/subsequent recrystallization process. According to the Particle Stimulated Nucleation (PSN) theory, these small dispersed particles inhibit the movement of dislocation and sub-grain boundaries, hindering the nucleation and growth of recrystallized grains [14]. Due to the non-uniformity of rolling deformation, recrystallization nucleation and growth occur at the sites with large deformation energy storage, and the growth occurs by engulfing small crystal grains around. Consequently, obtains coarse recrystallization grain. From Fig. 3(b), the homogeneously annealed sample at 590°C contains large-sized particles. During the subsequent annealing, the particles grow and more and more particles are larger than 1 μm. According to the PSN theory, large particles($>1\mu$m) exacerbate local cold deformation, increase deformation storage energy, promote nucleation, and refine grains. Thus, small equiaxed grains are obtained.

In addition to the size factor of the second phase, the interaction of the second phase precipitation with the recrystallization process also has an important effect on the recrystallization process and microstructure [14]. In supersaturated Al-Mn alloys, precipitation occurs before or simultaneously with recovery and recrystallization which is referred to as concurrent precipitation [19]. The interaction between precipitation and recrystallization mainly depends on the critical Tc. When T>Tc, recrystallization is slightly affected by precipitation, and when T<Tc, concurrent precipitation inhibits recovery and recrystallization. For the Sample A, the final annealing temperature T<Tc. Therefore, the material obtains large pancake-like grains. For the Sample B, the final annealing temperature T>Tc. Thus, fine equiaxed grains are obtained.

The melting clad alloy penetrates into the core alloy along the grain boundaries, reducing the brazability of multi-layers brazing sheets. The grain boundary is considered to be a

high-speed diffusion channel. During brazing, Si in the elongated grains travel much longer through the same depth compared to equiaxed grains. Therefore, the barriers and diffusion activation energy are much larger than that in fine equiaxed grains, and diffusion will also be much more difficult. From Fig. 5, the Si content of the diffusion zone of the non-homogeneously annealed material increased only by 0.2 w.t %, while the Si content of the diffusion zone of the homogeneous material increased by 0.6 wt. %.

Mn in the core material exists as dispersoids and solid solution in the matrix. The amount of Mn in the solid solution for processing B before brazing is 0.44 wt. %. The amount of Mn in the solid solution for processing A before brazing can be as high as 0.89 wt. %, which indicates its supersaturation. After brazing the alloy is at 600 °C, Si diffuses from the clad alloy into the core alloy. Si will make the supersaturated solid solution of Mn unstable and will force Mn and Fe to precipitate as α-Al(Fe,Mn)Si [9]. BDP formed in the diffusion zone, as shown in Fig. 2(c). The formation of BDP and the depletion of manganese in the solid solution are responsible for the enhanced corrosion resistance of aluminum brazing sheet.

B. DIFFUSION OF Si

When $T<0.5\ T_m \sim 0.75\ T_m$ (Tm is the equilibrium melting temperature), diffusivity at the grain boundary regions is higher than in the bulk material, and D_{gb}/D_l is 10^5 or higher [20]. D_{gb} is the grain boundary diffusion coefficient; D_l is the lattice diffusion coefficient.

The final annealing temperature for process A and process B is 420°C, and T/Tm is approximately 0.65. Therefore, diffusivity of Si at the grain boundary regions is higher than in the bulk material. Samples for process B is composed of fine equiaxed grains, so the diffusion depth of Si in the sample B is significantly deeper than in the sample A.

The brazing temperature of processing A and processing B is 600°C, and T/Tm is approximately 0.93. Thus, diffusivity of Si in the grain boundary regions is relatively small. Therefore, the diffusion solidification in sample A is similar to that in the sample B. However, as can be seen from Fig. 5, the diffusion depth of Si in the sample B after brazing is significantly deeper than that in the sample A.

During the brazing process, the liquid clad layer penetrates into the core layer along the grain boundaries. The driving force of this migration is the interfacial energy:

$$F = \gamma_{GB} - 2\gamma_{SL} \tag{2}$$

The grain boundary energy of the high-angle grain boundary is much higher than that of the low-angle grain boundary [20]. Only grain boundaries with a misorientation of 15° or higher will be wetted. This means that Si from the clad alloy penetrates only along the high angle grain boundaries. The fraction of the high-angle grain boundary fraction in sample B is larger than in sample A. Therefore, the penetration speed of Si in the sample B was faster than in the sample A. Thus, the core layer with pancake-like grains can limit diffusional solidification and extend the retention time of the melt clad.

Besides, gradient distribution of Si from the clad to core is formed in the sample B after brazing. Sample A has no significant concentration gradient due to the formation of the DBP region in the diffusion region.

C. CORROSION MECHANISM

The alloying elements Cu and Si have an important influence on the corrosion potential and corrosion resistance of AA4343/3z23a/AA4343 brazing sheet. Si has an ennobling effect on the corrosion potential of the aluminum matrix, which will increase the OCP values which are measured in the affected area. Cu in solid solution increases the OCP values measured in the diffusion zone and the local corrosion resistance [21]. Thus, diffusion of Si from the clad to the core reduces the corrosion potential of the clad material, but the copper diffusion has a greater influence on the corrosion potential than Si [15]. From Fig. 6, the nobler OCP of the clad material with homogenization for the brazed material can be attributed to Cu diffusion into the clad material. The electrochemical effect of Cu and Si diffusion during homogenization is 10-mV increase of the OCP for the clad material.

From Fig. 7(a) and (b), the interfacial region between the re-solidified clad material and the core material exhibits the highest density of precipitates. The Al(Fe,Mn)Si precipitates are the cathode compared to the Al matrix, which allow for galvanic coupling and corrosion propagation between the Al matrix and the precipitates [22]. The high density of Al(Fe,Mn)Si cathode precipitates promote dissolution of the Al matrix around them and causes corrosion propagation along the clad layer. The formation of BDP and the depletion of manganese in the solid solution avoid perforation corrosion and are considered to be responsible for the enhanced corrosion resistance of the aluminum brazing sheet [23].

The electrochemical depth profiling of aluminium brazing sheet for processing A after brazing are schematically shown in Fig. 9(a). Since the solid solution Mn content in the core material is high, it has a high corrosion potential. The corrosion potential of the core material is -680 mV, and corrosion potential of the re-solidified clad is -688 mV, which is slightly higher than diffusion zone (-694 mv) because it contains less copper and less manganese. As can be seen in Fig. 9(a), the corrosion potential difference between re-solidified clad and the core alloy is 14 mV. Besides, the diffusion zone contains large quantities of Al(FeMn),Si precipitates, which are cathode phase with respect to Al matrix, which makes the diffusion region susceptible to corrosion. When the corrosion spread to the BDP, the corrosion form is replaced by exfoliation corrosion due to the lower corrosion potential of high density of Al(Fe,Mn)Si precipitates. This means that when most of the diffusion zone has been corroded, corrosion of the re-solidified clad layer is the next step. When both the diffusion zone and the resolidified clad layer have corroded, subsequent corrosion of the core layer occurs. The BDP acted as an active cathode and avoid perforation corrosion of

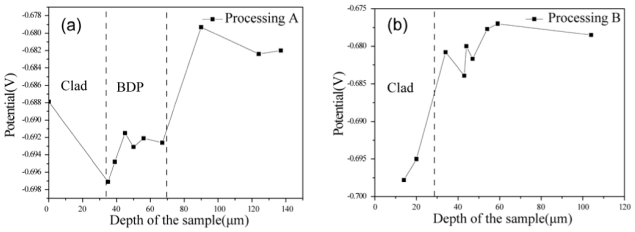

FIGURE 9. The electrochemical depth profiling of aluminium brazing sheet after brazing.

aluminium brazing sheets, which greatly improve the corrosion life of the material as well as the perforation time.

The electrochemical depth profiling of aluminium brazing sheet for processing B after brazing are schematically shown in Fig. 9(b). As can be seen in Fig. 9(b), the corrosion potential difference between resolidified clad layer and the core layer is 20 mV. Corrosion of the core layer is the next step when most of the resolidified clad layer has been corroded. From many points of clad penetration, corrosion proceed in all directions, which is often referred to as pitting of the core. This leads to a quick perforation of the brazing sheets. The progress of the corrosion in sample B after penetration of the clad can be easily explained by the OCP which is represented in Fig. 9(b). Both the core and the re-solidified clad are then exposed to the corrosive environment. Due to the low OCP, the re-solidified clad preferentially corrode.

V. CONCLUSION

Applying EPMA and potentiodynamic polarization measurements, microstructural characterization, and electrochemical characterization of AA4343/3z23a/AA4343 layered aluminum sheets before and after brazing were studied. The following results can be drawn.

(1) Small and dispersed second phase particles in the non-homogeneous annealing sample inhibit the movement of dislocation and sub-grain boundaries, hinder the nucleation and growth of recrystallized grains, and lead to coarse recrystallization grains. The homogeneously annealed sample contains large-sized particles. During the subsequent annealing, the particles serve as a nucleation substrate for recrystallized grains to promote nucleation, lead to small equiaxed recrystallization grains.

(2) The fluidity of the brazing layer without homogenization is significantly better than that with homogenization.

(3) The Si concentration of the affected area significantly increases after brazing. For the homogenization annealed samples, the Cu in the core layer diffuses into the clad layer and the Cu concentration of re-solidified clad increases significantly.

(4) The band of dense precipitates, formed in the diffusion zone during brazing, changes the corrosion mechanism of the Al brazing sheets from inter-granular corrosion to local exfoliation corrosion, which greatly improves the corrosion life of the brazing sheets as well as the perforation time.

REFERENCES

[1] R. K. Gupta, C. Li, J. Xia, X. Zhou, G. Sha, B. Gun, S. P. Ringer, and N. Birbilis, "Corrosion behaviour of Al–4Mg–1Cu (wt%) microalloyed with Si and Ag," *Adv. Eng. Mater.*, vol. 17, pp. 1670–1674, Nov. 2016.

[2] Y. Li, N. Tan, Z. Xu, Z. Luo, K. Han, Q. Zhai, and H. Zheng, "Enhancement of fatigue endurance by Al-Si coating in hot-stamping boron steel sheet," *Metals*, vol. 9, no. 7, p. 722, 2019.

[3] Y. Shi, L. Shao, J. Huang, and Y. Gu, "Effects of Si and Mg elements on the microstructure of aluminum–steel joints produced by pulsed DE-GMA welding–brazing," *Mater. Sci. Technol.*, vol. 29, no. 9, pp. 1118–1124, 2013.

[4] W. Zhang, T. Jin, W. Lou, W. Li, and W. Dai, "Mechanical properties and corrosion behavior of 5A06 alloy in seawater," *IEEE Access*, vol. 6, pp. 24952–24961, 2018.

[5] O. Engler and J. Hirsch, "Texture control by thermomechanical processing of AA6xxx Al–Mg–Si sheet alloys for automotive applications—A review," *Mater. Sci. Eng., A*, vol. 336, pp. 249–262, Oct. 2002.

[6] H. Inoue, T. Yamasaki, G. Gottstein, P. Van Houtte, and T. Takasugi, "Recrystallization texture and r-value of rolled and T4-treated Al-Mg-Si alloy sheets," *Mater. Sci. Forum*, vols. 495–497, pp. 573–578, Sep. 2005.

[7] J. Sidor, A. Miroux, R. Petrov, and L. Kestens, "Controlling the plastic anisotropy in asymmetrically rolled aluminium sheets," *Philos. Mag.*, vol. 88, pp. 3779–3792, Oct. 2008.

[8] J. J. Sidor, R. H. Petrov, and L. A. I. Kestens, "Modeling the crystallographic texture changes in aluminum alloys during recrystallization," *Acta Mater.*, vol. 59, pp. 5735–5748, Aug. 2011.

[9] Y. J. Li and L. Arnberg, "Quantitative study on the precipitation behavior of dispersoids in DC-cast AA3003 alloy during heating and homogenization," *Acta Mater.*, vol. 51, pp. 3415–3428, Jul. 2003.

[10] T. A. Bennett, R. H. Petrov, L. A. I. Kestens, L.-Z. Zhuang, and P. D. Smet, "The effect of particle-stimulated nucleation on texture banding in an aluminium alloy," *Scripta Mater.*, vol. 63, pp. 461–464, Sep. 2010.

[11] Y. J. Li and L. Arnberg, "Evolution of eutectic intermetallic particles in DC-cast AA3003 alloy during heating and homogenization," *Mater. Sci. Eng., A*, vol. 347, pp. 130–135, Apr. 2003.

[12] S. Tangen, K. Sjølstad, T. Furu, and E. Nes, "Effect of concurrent precipitation on recrystallization and evolution of the P-texture component in a commercial Al-Mn alloy," *Metall. Mater. Trans. A*, vol. 41A, pp. 2970–2983, Nov. 2010.

[13] H. E. Vatne, O. Engler, and E. Nes, "Influence of particles on recrystallisation textures and microstructures of aluminium alloy 3103," *Mater. Sci. Technol.*, vol. 13, no. 2, pp. 93–102, 2013.

[14] F. J. Humphreys and M. Hatherly, *Recrystallization and Related Annealing Phenomena*, 2nd ed. Amsterdam, The Netherlands: Elsevier, 2004.

[15] F. N. Afshar, J. H. W. de Wit, H. Terryn, and J. M. C. Mol, "The effect of brazing process on microstructure evolution and corrosion performance of a modified AA4XXX/AA3XXX brazing sheet," *Corrosion Sci.*, vol. 58, pp. 242–250, May 2012.

[16] F. N. Afshar, F. D. Tichelaar, A. M. Glenn, P. Taheri, M. Sababi, H. Terryn, and J. M. C. Mol, "Improved corrosion resistance of aluminum brazing sheet by a post-brazing heat treatment," *Corrosion*, vol. 73, pp. 379–393, Apr. 2017.

[17] S. Iwao, S. Kuroda, and M. Asano, "Effects of Cu content in the core, Zn in the filler, and sheet thickness on the corrosion resistance of a brazing sheet," *Weld. Int.*, vol. 23, no. 12, pp. 886–894, 2009.

[18] F. N. Afshar, E. Szala, A. Wittebrood, R. Mulder, J. M. C. Mol, H. Terryn, and J. H. W. de Wit, "Influence of material related parameters in sea water acidified accelerated test, reliability analysis and electrochemical evaluation of the test for aluminum brazing sheet," *Corrosion Sci.*, vol. 53, no. 12, pp. 3923–3933, Dec. 2011.

[19] M. Somerday and F. J. Humphreys, "Recrystallisation behaviour of supersaturated Al–Mn alloys Part 1—Al–1.3 wt-%Mn," *Mater. Sci. Technol.*, vol. 19, pp. 20–29, Jan. 2003.

[20] Y. Tu, Z. Tong, and J. Jiang, "Effect of microstructure on diffusional solidification of 4343/3005/4343 multi-layer aluminum brazing sheet," *Metall. Mater. Trans. A*, vol. 44, no. 4, pp. 1760–1766, Apr. 2013.

[21] T. Suter and R. C. Alkire, "Microelectrochemical studies of pit initiation at single inclusions in Al 2024-T_3," *J. Electrochem. Soc.*, vol. 148, pp. B36–B42, Jan. 2001.

[22] K. Bordo, V. C. Gudla, L. Peguet, A. Afseth, and R. Ambat, "Electrochemical profiling of multi-clad aluminium sheets used in automotive heat exchangers," *Corrosion Sci.*, vol. 131, pp. 28–37, Feb. 2018.

[23] F. N. Afshar, J. H. W. de Wit, H. Terryn, and J. M. C. Mol, "Scanning Kelvin probe force microscopy as a means of predicting the electrochemical characteristics of the surface of a modified AA4xxx/AA3xxx (Al alloys) brazing sheet," *Electrochimica Acta*, vol. 88, pp. 330–339, Jan. 15 2013.

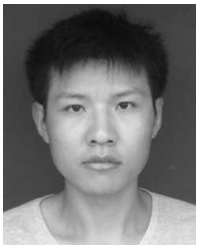

ZHIPENG YUAN received the B.S. and M.S. degrees in materials science and engineering from Henan Polytechnic University, Jiaozuo, China, in 2017. He is currently pursuing the Ph.D. degree in materials science and engineering with Southeast University, Nanjing, China. His research interests include the influencing factors of erosion and corrosion resistance of aluminum brazing sheets.

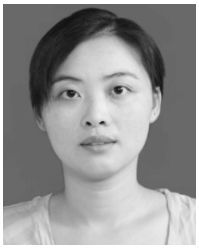

FANGYUN TAO received the B.S., M.S., and Ph.D. degrees from Southeast University, China. Her research interests include study on total arboricity and list total arboricity of graphs.

JIE WEN received the B.S. degree in materials science and engineering from the Yancheng Institute of Technology, Yancheng, China, in 2017. He is currently pursuing the M.S. degree in materials science and engineering with Southeast University, Nanjing, China. His research interests include effect of two-stage annealing on microstructure and mechanical properties of AA3xxx aluminum alloy sheet.

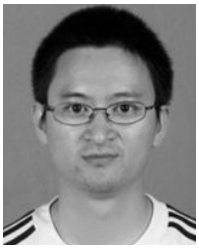

YIYOU TU received the B.S., M.S., and Ph.D. degrees from Southeast University, China, where he is currently an Associate Professor. His research interests include study on preparation and properties of high performance special steel materials, development of ultrahigh conductivity aluminum conductor, and study on the control of grain boundary distribution of aluminum alloy.